Journal of Colloid and Interface Science 484 (2016) 249–253

Contents lists available at ScienceDirect

Journal of Colloid and Interface Science

journal homepage: www.elsevier.com/locate/jcis

Regular Article

Relative adsorption excess of ions in binary solvents determined by grazing-incidence X-ray fluorescence

Monika Witala [a], Oleg Konovalov [b], Kim Nygård [a,*]

[a] Department of Chemistry and Molecular Biology, University of Gothenburg, SE-41296 Gothenburg, Sweden
[b] European Synchrotron Radiation Facility, 71 Avenue des Martyrs, F-38000 Grenoble, France

GRAPHICAL ABSTRACT

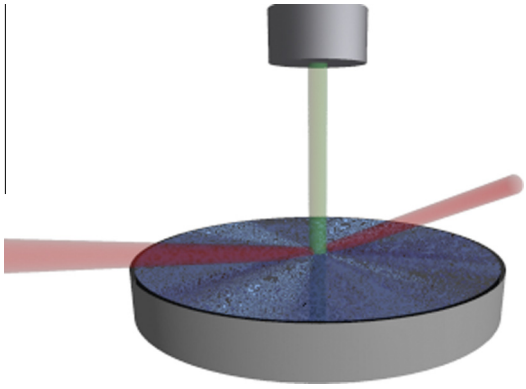

ARTICLE INFO

Article history:
Received 8 June 2016
Revised 1 September 2016
Accepted 2 September 2016
Available online 4 September 2016

Keywords:
Adsorption excess
Binary aqueous solvents
Grazing-incidence X-ray fluorescence

ABSTRACT

We demonstrate a model-independent method for experimental determination of the relative surface excess of inorganic ions in binary liquid mixtures, based on grazing-incidence X-ray fluorescence. For this purpose, we probe the ion density profiles in a mixture of water and 2,6-dimethylpyridine containing a hydrophilic salt, potassium chloride. Thereby we demonstrate that the proposed method quantifies in a direct manner the difference between cation and anion excess adsorption in binary solvents with a resolution of one excess ion per 200 nm^2 or better.

1. Introduction

The surface composition of solutions is an important problem within the field of colloid and interface science. Traditionally it is described in terms of Gibbs adsorption isotherm, a very fundamental concept first derived by Gibbs [1,2]. This well know relation binds the surface tension (γ) with the chemical potential (μ) at the equilibrium states of all chemical species in the system,

$$-d\gamma = \sum_i \Gamma_i d\mu_i. \quad (1)$$

The third term, the so-called excess adsorption Γ_i, gives the surface composition in terms of an excess adsorption of each specie i with respect to its bulk concentration, and it can be either positive or

* Corresponding author.
E-mail address: kim.nygard@chem.gu.se (K. Nygård).

http://dx.doi.org/10.1016/j.jcis.2016.09.005
0021-9797/

negative depending on the nature of the ith component. For example, surfactants added to water adsorb at the liquid surface, giving a positive Γ. This is in contrast to simple inorganic salts, which are depleted from the interfacial region, resulting in negative values of Γ.

Eq. (1) provides a conceptually straightforward approach to experimentally determine the surface composition; by measuring the surface tension as a function of chemical potential (in practice activity or concentration), one can determine the net excess adsorption. However, in this process one has to define the Gibbs dividing surface, the exact placement of which affects the values of Γ_i. In two-component systems it is convenient to use the relative surface excess Γ_2^1 of the solute (2) with respect to the solvent (1), by placing the dividing surface between liquid and vapor phases such that $\Gamma_1 = 0$ for the solvent. Measurement of the surface tension then yields the excess adsorption, thus capturing the adsorption or depletion of solutes [3–6].

For multi-component systems the situation is not as straightforward. Considering binary solvents, for example, one would need to know the interfacial concentration distributions of both solvent components in order to set $\Gamma_{\text{solvent}} = 0$ as a reference. For such solvents surface tension measurements are not a convenient approach to determine the solutes' excess adsorption, and other methods must be developed. However, to date only a few alternative approaches for determining Γ values have been reported. The radiotracer technique is an early example [7,8], which is hampered by experimental challenges and inaccuracy. Surface-sensitive optical techniques such as ellipsometry can be employed, although the data are not straightforwardly related to the surface excess [9,10]. In principle the surface composition could be determined at molecular scale using X-ray reflectivity [11], but the method would rely on modeling of the concentration profiles. Neutron reflectivity using isotope substitution, where the solvent is made 'invisible', provides the excess adsorption in a model-independent manner [12,13], but the approach is challenging for multi-component solvents. For a comprehensive review on alternative methods, see Ref. [14]. Clearly, the number of techniques directly probing solute species in a mixed solvent is limited.

In this article, we present a method for direct experimental determination of the relative surface excess of solute species in binary solvents, which does not depend on modeling of concentration profiles. We demonstrate the method by probing ion density profiles at the liquid-vapor interface using grazing-incidence X-ray fluorescence (GIXF, see Fig. 1), thereby determining the difference between cation and anion excess adsorption in a direct, model-independent manner. Following our recent work [15] the binary mixture is composed of water and 2,6-dimethylpyridine (denoted 2,6-DMP) with 10 mM added potassium chloride (KCl). For a schematic view of our system, see Fig. 2. Most importantly, we demonstrate that GIXF can probe differences in the ions' surface excess with a resolution of one excess ion per 200 nm^2 or better.

2. Materials and methods

2.1. Materials

Following Ref. [15], the studied sample was composed of a binary liquid mixture of water (Millipore) and 2,6-DMP (Sigma-Aldrich, purity $\geqslant 99\%$) with a 2,6-DMP volume fraction of $\phi = 0.3$. As added salt we used potassium chloride (Sigma-Aldrich, purity $\geqslant 99\%$). All chemicals were used without further purification.

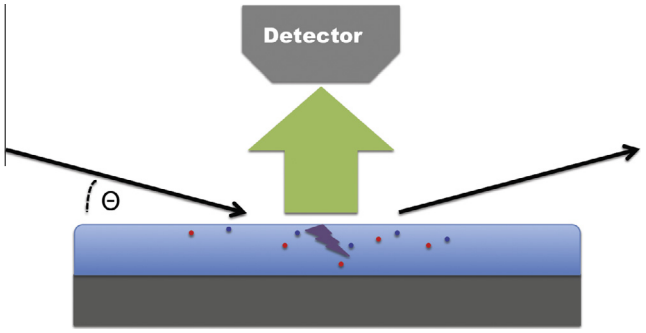

Fig. 1. A schematic layout of the setup in the GIXF experiment. Black arrows represent the incident and reflected X-ray beams. The incoming beam hits the liquid-vapor interface under shallow angles θ, causing an evanescent wave (purple symbol) to penetrate the liquid surface and excite the ionic species present in the liquid sample, K^+ and Cl^- in this study. The green wide arrow shows the fluorescence emitted by the ions. (For interpretation of the references to colour in this figure legend, the reader is referred to the web version of this article.)

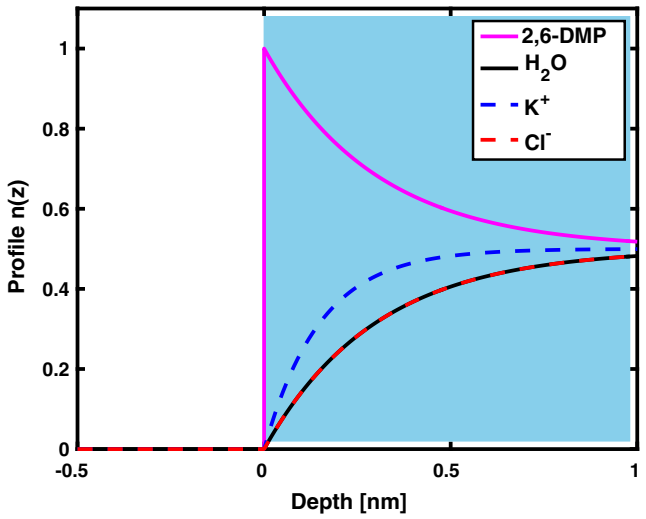

Fig. 2. Schematic normalized density profiles at the liquid-vapor interface, with the white and light blue regions depicting the vapor and liquid phases, respectively. Profiles are shown for water (black solid line), 2,6-DMP (magenta solid line), potassium (blue dashed line), and chloride (red dashed line). (For interpretation of the references to colour in this figure legend, the reader is referred to the web version of this article.)

2.2. Sample cell

We kept the sample in a steel dish (diameter ≈100 mm, depth 2 mm) placed in a custom-made cylindrical sample cell. The sample cell had large entrance and exit windows made of Kapton, the latter allowing us to monitor the specular X-ray reflectivity. Moreover, the cell had an opening on the top for the fluorescence detector. We kept the temperature of the sample stable within ≈ 0.1 K using a chiller (Julabo) connected to the sample cell. See Fig. 3 for a picture of the sample cell.

2.3. GIXF experiment

We carried out the GIXF experiment at the beamline ID10 of the European Synchrotron Radiation Facility (ESRF, France), using an incident X-ray energy of 8 keV. We collected data at several temperatures ($T \approx 295 \ldots 301$ K) and we kept the sample under helium atmosphere in order to reduce parasitic argon fluorescence from air. We recorded the fluorescence spectra using the Vortex

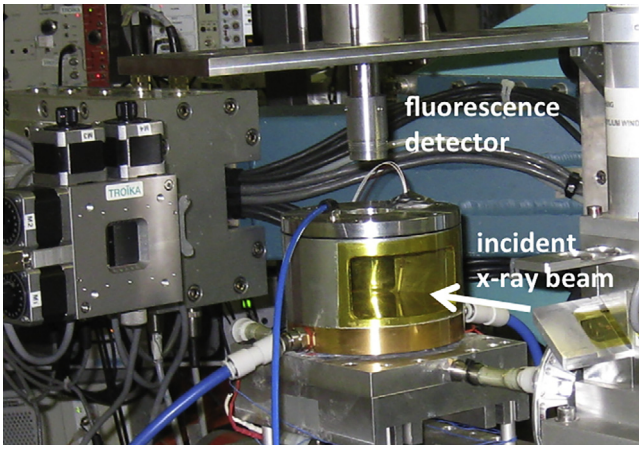

Fig. 3. Cylindrical sample cell with Kapton windows used in the experiment. The incident X-ray beam enters from the right, as shown by the arrow. During the experiment the fluorescence detector is lowered close to the liquid surface.

energy-dispersive detector (SII NanoTechnology), which we placed ≈20 mm above the liquid surface in order to maximize the solid angle of detection. For alignment and monitoring purposes, we also measured the specular X-ray reflectivity from the liquid-vapor interface using the VÅNTEC-1 detector (Bruker). The GIXF technique has been described elsewhere [16,17]. For a recent review on the technique, see Ref. [18].

2.4. Data analysis

We carried out all data reduction and analysis in MATLAB (MathWorks).

3. Results and discussion

3.1. Grazing-incidence X-ray fluorescence

In order to determine the near-surface composition we carried out a GIXF experiment (see Fig. 1 for a schematic), which allows to distinguish cations and anions through element-specific fluorescence emission. In GIXF the incident X-ray beam hits the liquid-vapor interface at a grazing angle, inducing the propagation of an evanescent wave in the sample. The evanescent wave, in turn, causes excitement of ions and ensuing fluorescence emission. By varying the angle of incidence θ we tune the evanescent wave propagation in the sample and thus the depth of probing, yielding depth-dependent data. Below the critical angle of total reflection θ_C (0.152° in the present experiment) the cation and anion distributions are probed within ≈5 nm from the surface, whereas by increasing the incident angle to a larger value than θ_C one measures the bulk.

Formally the fluorescence intensity as a function of incidence angle is described by

$$I_{\pm}(\theta) = C_{\pm}(\theta)\int_0^{\infty} I_0(z,\theta)n_{\pm}(z)\exp(-\mu_{\pm}z)dz. \quad (2)$$

We have defined the z axis normal to the surface and assumed the liquid-vapor interface to be at $z = 0$, with the liquid phase at $z \geqslant 0$. [1] Here $I_0(z,\theta)$ is the intensity distribution of X-rays in the sample (the so-called illumination profile), $n_{\pm}(z)$ the ion number density profiles, and $\mu_{\pm}$ the tabulated [20] linear absorption coefficients for the ions' fluorescence lines in the solvent. The other factors, such as acceptance angle and quantum efficiency of the detector, do not depend on the ion distributions in the sample and have been included in the prefactor $C_{\pm}(\theta)$. Eq. (2) provides a relation between the GIXF intensity $I_{\pm}(\theta)$ and the ion number density profile $n_{\pm}(z)$, and hence means to experimentally verify theoretical predictions of the ions' near-surface composition. This was indeed the approach in our previous study on salt-containing binary solvents [15]. Here we will demonstrate that the experimental GIXF data also provide useful information on surface adsorption in a direct manner, without the need of modeling.

GIXF has already been applied for pioneering surface composition studies of alkali-halide salts in aqueous solutions [21], providing the excess adsorption from recorded GIXF intensities. Moreover, by considering relative GIXF intensities one can minimize systematic errors due to the prefactor $C(\theta)$ of Eq. (2) [15,22]. Here we combine these two approaches in order to determine the relative excess adsorption $\Delta\Gamma \equiv \Gamma_+ - \Gamma_-$ from the experimental data in a direct, model-independent manner. In practice, we follow the idea proposed by Padmanabhan and co-workers [21], who expanded the normalized GIXF intensity of Eq. (2) in terms of the effective inverse penetration depth $\alpha_{\pm}$ as

$$I_{\pm}(\theta) \propto 1 + \frac{\alpha_{\pm}(\theta)\Gamma_{\pm}}{n^0_{\pm}} - \frac{\alpha^2_{\pm}(\theta)}{n^0_{\pm}}\int_0^{\infty}[n_{\pm}(z) - n^0_{\pm}]zdz + \mathcal{O}[\alpha^3_{\pm}(\theta)], \quad (3)$$

where $\Gamma_{\pm} = \int_0^{\infty}[n_{\pm}(z) - n^0_{\pm}]dz$ is the excess adsorption, $n^0_{\pm}$ the bulk ion number density, and $\alpha_{\pm} = 2\mathrm{Im}[k_z(\theta)] + \mu_{\pm} \equiv \alpha + \mu_{\pm}$ with k_z the normal component of the incident wave vector in the liquid phase, while $\mathcal{O}$ represents higher-order corrections (α is readily calculated [11] using tabulated optical constants [23]). Here we have for clarity stated the θ dependence explicitly, but it is implicitly assumed throughout the paper. Note that since the effective penetration depth is much larger than the characteristic length of the ion distributions, we can neglect the third term and higher-order corrections in the right-hand side of Eq. (3). Below the critical angle for total reflection, $\theta < \theta_C$, the effective inverse penetration depth is dominated by the decay of the illumination profile, $1/\alpha \approx 5$ nm, and we may set $\alpha_+ \approx \alpha_- \approx \alpha$. For a symmetric electrolyte we further have $n^0_+ = n^0_- = n_0$, leading to the relative GIXF intensity

$$\frac{I_+}{I_-} \approx \frac{1 + \alpha\Gamma_+/n_0}{1 + \alpha\Gamma_-/n_0}. \quad (4)$$

From Eq. (4) we can finally obtain the relative adsorption excess as

$$\Delta\Gamma \equiv \Gamma_+ - \Gamma_- \approx \left(\frac{n_0}{\alpha} + \Gamma_-\right)\left(\frac{I_+}{I_-} - 1\right) \approx \frac{n_0}{\alpha}\left(\frac{I_+}{I_-} - 1\right). \quad (5)$$

In the last part we have used the result $n_0/\alpha \gg |\Gamma_-|$, which is valid when the effective inverse penetration depth (≈5 nm) is much larger than the range of inhomogeneities in $n_-(z)$. Eq. (5) is the main result of the present paper, showing that $\Delta\Gamma$ can be obtained directly from the experimentally measured relative GIXF intensity I_+/I_- without any modeling.

3.2. GIXF experiment

In order to demonstrate the method for determining $\Delta\Gamma$ outlined above, we apply it to a mixture of water and 2,6-DMP containing 10 mM KCl. It has previously been found that 2,6-DMP adsorbs at the liquid surface of this particular binary liquid mixture [24]. Because of asymmetric solvation preferences of the ions [25] one expects microscopic charge segregation, with the strongly hydrophilic anions being expelled more strongly from the interface than the weakly hydrophilic cations. This picture is schematically presented in Fig. 2. Such a relative excess of cations compared to

[1] Within the angular range of the GIXF experiment, we are not sensitive to the roughness [19] of the liquid surface.

anions near the interface is expected to show up in the GIXF data, as was indeed observed by us in a recent study [15].

In Fig. 4 we present typical fluorescence spectra showing Kα and Kβ lines of K^+ (~3.3 keV and ~3.6 keV) and Cl^- (~2.6 keV and ~2.8 keV). Data are presented for incidence angles both below ($\theta = 0.07°$) and above ($\theta = 0.17°$) the critical angle ($\theta_c = 0.152°$), and the former data have been rescaled and offset vertically to facilitate comparison. We note two important observations. First, the simultaneous measurement of K^+ and Cl^- fluorescence allows us to determine the relative GIXF intensity I_+/I_-, and hence to determine the relative adsorption excess $\Delta\Gamma$ using Eq. (5). Second, the fluorescence lines are well separated from the background even for $\theta < \theta_c$, implying that these experiments can be extended to smaller salt concentrations than the 10 mM used here.

Following Ref. [26], we reduced the measured fluorescence spectra by subtracting a linear background and fitting one Gaussian function to each fluorescence peak (black lines in Fig. 4). In order to minimize the number of free parameters we used tabulated, element-specific values for the fluorescence peak positions and the relative intensities of Kα to Kβ fluorescence [27]. By monitoring the K^+ and Cl^- Kα intensities as a function of incidence angle θ, normalizing the data at large θ (which are proportional to the bulk ion concentrations), and taking their ratio, we finally obtain the relative GIXF data of Fig. 5 collected at several temperatures in the range ≈ 295 . . . 301 K. Importantly, the relative GIXF intensity I_+/I_- is larger than unity for angles smaller than the critical angle, i.e. $\theta < \theta_C$, demonstrating the excess of cations compared to anions near the interface [15]. The same effect is observed for all temperatures studied here.

3.3. Relative ion adsorption excess

Finally, we are in the position to estimate the relative surface excess between K^+ and Cl^- ions, $\Delta\Gamma$. By applying Eq. (5) on the experimental data of Fig. 5 in the range $\theta < \theta_C$, we obtain $\Delta\Gamma = (9.6 \pm 5.2) \times 10^{15}, (3.3 \pm 1.1) \times 10^{15}$, and $(4.6 \pm 2.8) \times 10^{15}$ ions/m^2 at 295, 298 and 301 K, respectively. The resolution of the experiment is one excess ion per 200 nm^2 or better, similar to previous GIXF studies on surface excess of ions [21]. To put this in perspective, for a dilute two-component system (solvent + solute) at room temperature, a surface excess Γ of one solute molecule per 200 nm^2 would correspond to a minute change of the surface tension, $|\Delta\gamma| \lesssim k_B T\Gamma \approx 0.02$ mN/m (with k_B denoting Boltzmann's constant), highlighting the sensitivity of the GIXF technique.

In practice, GIXF is applicable to elements in the third and higher periods. As a consequence we were not directly sensitive to the distribution of solvent components, H_2O and 2,6-DMP, and were limited to the relative ion excess $\Delta\Gamma$. A possible improvement would be to carry out simultaneous GIXF and X-ray reflectivity experiments, where the latter may be sensitive to the solvent structure. While the electron density contrast between H_2O and 2,6-DMP is too small for a meaningful X-ray reflectivity study, the technique may be sensitive to other solvent mixtures.

4. Conclusions and outlook

We report an experimental, model-independent approach for determining the relative adsorption excess of ions (or other solutes) at liquid surfaces based on element-specific grazing-incidence X-ray fluorescence. By measuring relative fluorescence intensities from a binary solvent of water and 2,6-DMP containing 10 mM potassium chloride, we demonstrate that the method is sensitive to one excess ion per ≈200 nm^2. The present scheme is complimentary to mature techniques such as ellipsometry [9,10] and neutron reflectivity [12–14], with the added value that it provides model-independent adsorption data also for multi-component solvents. We note, however, that the method can also readily be applied to single-component solvents.

Previous applications of grazing-incidence X-ray fluorescence to ion adsorption at liquid surfaces have focused on solute concentrations in the 100 mM range [21,22]. The data of Fig. 4 imply that the technique can now be extended towards salt concentrations as

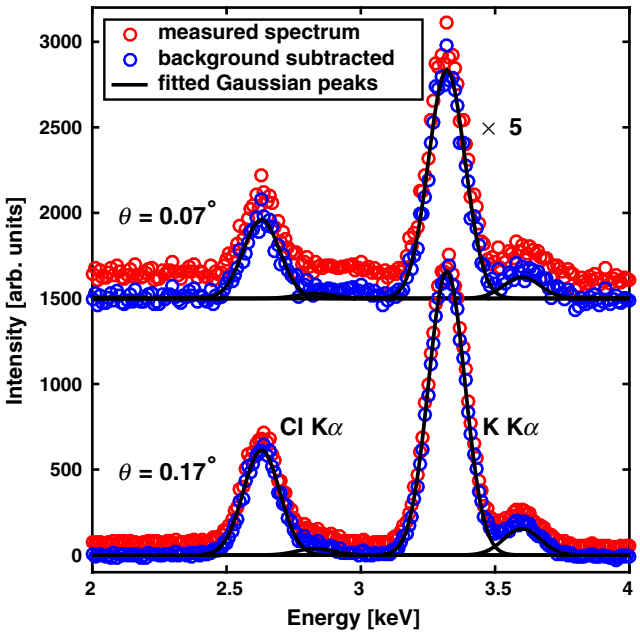

Fig. 4. Typical GIXF spectra measured from a mixture of water and 2,6-DMP containing 10 mM KCl, collected for incidence angles of $\theta = 0.07°$ and 0.17°. Red symbols show the measured spectra, blue symbols the data after subtracting a linear background, and black lines Gaussians fitted to the fluorescence signal of potassium (K^+ Kα ≈ 3.3 keV; K^+ Kβ ≈ 3.6 keV) and chloride (Cl^- Kα ≈ 2.6 keV; Cl^- Kβ ≈ 2.8 keV). The data for $\theta = 0.07°$ have been multiplied by a factor of five and offset vertically by 1500 units for clarity. (For interpretation of the references to colour in this figure legend, the reader is referred to the web version of this article.)

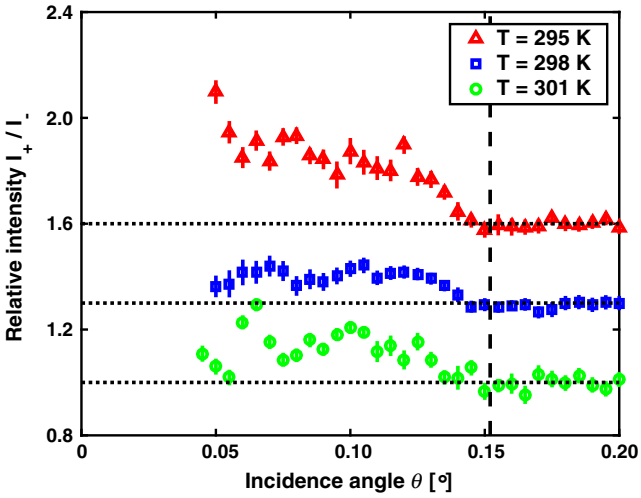

Fig. 5. Relative GIXF intensity I_+/I_- as a function of incidence angle θ for the mixture of water and 2,6-DMP containing 10 mM KCl. Experimental data are collected at several temperatures, $T = 295$, 298, and 301 K. The vertical dashed line represents the critical angle of total reflection θ_C in this experiment. The two upper curves are shifted vertically by a constant (blue squares by 0.3 and red triangles by 0.6) for clarity. The dotted horizontal lines indicate unity for each data set. (For interpretation of the references to colour in this figure legend, the reader is referred to the web version of this article.)

small as ≈1 mM – a highly relevant concentration regime for applications within the field of colloid and interface science. We believe grazing-incidence X-ray fluorescence will prove particularly useful when addressing surface adsorption in solute-containing liquid mixtures, i.e., when studying complex multi-component systems where one can fully exploit the element specificity of the technique.

Acknowledgments

We thank the European Synchrotron Radiation Facility for providing beamtime and the Swedish Research Council (Grant No. 621-2012-3897) for financial support.

References

[1] J.W. Gibbs, On the equilibrium of heterogeneous substances, Trans. Conn. Acad. Arts Sci. 3 (1876) 108–248, 1878, 343–254.
[2] C.J. Radke, Gibbs adsorption equation for planar fluid-fluid interfaces: invariant formalism, Adv. Colloid Interface Sci 222 (2015) 600–614.
[3] A.J. Prosser, E.I. Franses, Adsorption and surface tension of ionic surfactants at the air-water interface: review and evaluation of equilibrium models, Colloid Surf. A 178 (2001) 1–40.
[4] F.M. Menger, S.A.A. Rizvi, Relationship between surface tension and surface coverage, Langmuir 27 (2011) 13975–13977.
[5] R.I. Slavchov, J.K. Novev, Surface tension of concentrated electrolyte solutions, J. Colloid Interface Sci 387 (2012) 234–243.
[6] A.A. Shah, K. Ali, S. Bilal, Surface tension, surface excess concentration, enthalpy and entropy of surface formation of aqueous salt solutions, Colloid Surf. A 417 (2013) 183–190.
[7] J.K. Dixon, A.J. Weith, A.A. Argyle, D.J. Salley, Measurement of the adsorption of surface-active agent at a solution-air interface by a radiotracer method, Nature 163 (1949) 845.
[8] G. Aniansson, O. Lamm, A radioactive method for measuring the adsorption of dissolved substances on liquid surfaces, Nature 165 (1950) 357–358.
[9] C.D. Bain, Studies of adsorption at interfaces by optical techniques: ellipsometry, second harmonic generation and sum-frequency generation, Curr. Opin. Colloid Interface Sci. 3 (1998) 287–292.
[10] T. Battal, G.C. Shearman, D. Valkovska, C.D. Bain, R.C. Darton, J. Eastoe, Determination of the dynamic surface excess of a homologous series of cationic surfactants by ellipsometry, Langmuir 19 (2003) 1244–1248.
[11] J. Daillant, A. Gibaud (Eds.), X-ray and Neutron Reflectivity: Principles and Applications, Springer, Berlin Heidelberg, 2009.
[12] Z.X. Li, J.R. Lu, R.K. Thomas, Neutron reflectivity studies of the adsorption of Aerosol-OT at the air/water interface: the surface excess, Langmuir 13 (1997) 3681–3685.
[13] P.X. Li, Z.X. Li, H.-H. Shen, R.K. Thomas, J. Penfold, J.R. Lu, Application of the Gibbs equation to the adsorption of nonionic surfactants and polymers at the air-water interface: comparison with surface excess determined directly using neutron reflectivity, Langmuir 29 (2013) 9324–9334.
[14] J.R. Lu, R.K. Thomas, J. Penfold, Surfactant layers at the air water interface: structure and composition, Adv. Colloid Interface Sci. 84 (2000) 143–304.
[15] M. Witala, R. Nervo, O. Konovalov, K. Nygård, Microscopic segregation of hydrophilic ions in critical binary aqueous solvents, Soft Matter 11 (2015) 5883–5888.
[16] M.J. Bedzyk, G.M. Bommarito, J.S. Schildkraut, X-ray standing waves at a reflecting mirror surface, Phys. Rev. Lett. 62 (1989) 1376–1379.
[17] W.B. Yun, J.M. Bloch, X-ray near total external fluorescence method: experiment and analysis, J. Appl. Phys. 68 (1990) 1421–1428.
[18] E. Schneck, B. Demé, Structural characterization of soft interfaces by standing-wave fluorescence with X-rays and neutrons, Curr. Opin. Colloid Interface Sci. 20 (2015) 244–252.
[19] A. Braslau, P.S. Pershan, G. Swislow, B.M. Ocko, J. Als-Nielsen, Capillary waves on the surface of simple liquids measured by X-ray reflectivity, Phys. Rev. A 38 (1988) 2457–2470.
[20] I. Orlic, K.K. Loh, C.H. Sow, S.M. Tang, P. Thong, Parametrization of the total photon mass attenuation coefficients in the energy range 0.1–1000 keV, Nucl. Instr. Meth. Phys. Res. B 74 (1993) 352–361.
[21] V. Padmanabhan, J. Daillant, L. Belloni, S. Mora, M. Alba, O. Konovalov, Specific ion adsorption and short-range interactions at the air aqueous solution interface, Phys. Rev. Lett. 99 (2007) 086105.
[22] E. Schneck, T. Schubert, O.V. Konovalov, B.E. Quinn, T. Gutsmann, K. Brandenburg, R.G. Oliveira, D.A. Pink, M. Tanaka, Quantitative determination of ion distributions in bacterial lipopolysaccharide membranes by grazing-incidence X-ray fluorescence, Proc. Natl. Acad. Sci. U.S.A. 107 (2010) 9147–9151.
[23] B.L. Henke, E.M. Gullikson, J.C. Davis, X-ray interactions: photoabsorption, scattering, transmission, and reflection at $E = 50 - 30,000$ eV, $Z = 1 - 92$, At. Data Nucl. Data Tables 54 (1993) 181–342.
[24] J.H.J. Cho, B.M. Law, K. Gray, Strong critical adsorption at the liquid-vapor surface of a nonpolar mixture, J. Chem. Phys. 116 (2002) 3058–3062.
[25] H.D. Inerowicz, W. Li, I. Persson, Determination of the transfer thermodynamic functions for some monovalent ions from water to N,N-dimethylthioformamide, and for some anions from water to methanol, dimethyl sulfoxide, acetonitrile and pyridine, and standard electrode potentials of some $M^+/M(s)$ couples in N,N-dimethylthioformamide, J. Chem. Soc. Faraday Trans. 90 (1994) 2223–2234.
[26] W. Abuillan, E. Schneck, A. Körner, K. Brandenburg, T. Gutsmann, T. Gill, A. Vorobiev, O. Konovalov, M. Tanaka, Physical interactions of fish protamine and antisepsis peptide drugs with bacterial membranes revealed by combination of specular X-ray reflectivity and grazing-incidence X-ray fluorescence, Phys. Rev. E 88 (2013) 012705.
[27] R.B. Firestone, V.S. Shirley (Eds.), Tables of Isotopes, second ed., Wiley, New York, 1996, vol. II.